JOURNAL OF MATERIALS SCIENCE **36** (2001) 3395–3402

Effects of promoters on the product quality of nanophase SiC/α-Si_3N_4 composite powders synthesized through carbothermal reduction nitridation

KAREN J. BUECHLER, DAVID R. CHACON, DAVID R. SCOTT, ALAN W. WEIMER*
Department of Chemical Engineering, University of Colorado, Boulder, CO 80309-0424, USA
E-mail: alan.weimer@colorado.edu

The effect of additives is investigated for the carbothermal reduction synthesis of nanophase silicon carbide/silicon nitride composite powders. Mixtures of silica, carbon, seed silicon nitride, and additive are reacted in a thermogravimetric analyzer. The mass loss information combined with compositional and spectroscopic analysis allows product quality (morphology, surface area, α-Si_3N_4 and β-SiC contents, oxygen content, etc.) information to be obtained. It was observed that all of the additives used in this study increased the reaction rate. Lithium carbonate produced a silicon nitride/silicon carbide composite that was not significantly different from experiments without promoter. However, the product quality was severely affected in other instances.

1. Introduction and background

1.1. Si_3N_4 synthesis by carbothermal nitridation

In order for Si_3N_4 ceramics to compete in the engine components market, new powder syntheses are being researched in hopes of advancing an alternative method to meet the imposed cost requirements. It is advantageous to minimize the number of unit operations involved in the process, and to achieve as many of the required powder properties as possible during the synthesis step. Carbothermal synthesis (Equation 1) has attracted enormous interest because the process fulfills both of these criteria.

$$3SiO_{2(s)} + 6C_{(s)} + 2N_{2(g)} \rightarrow Si_3N_{4(s)} + 6CO_{(g)} \quad (1)$$

The biggest advantage to carbothermal nitridation is that if fine, high-surface area, high-purity SiO_2 and carbon are used, Si_3N_4, of the same quality, and with an α-phase content greater than 95%, is produced directly. This process does not necessitate a chemical intermediate, a crystallization step, or particle refinement. Although excess carbon is added to enhance the reducing environment, it is easily removed by heating the product in air at approximately 973 K. Excess carbon completely converts SiO_2 eliminating the need for acid leaching. Carbothermal synthesis uses readily available and relatively low cost starting materials. Their preparation cost is competitive, if not significantly lower, to that of starting materials used in other routes.

Another important feature of carbothermal nitridation is that nanophase SiC particles may be produced in-situ with Si_3N_4. Silicon nitride matrix composites with a dispersion of SiC nanoparticles can significantly enhance ductility, strength, and toughness compared to monolithic Si_3N_4 ceramics [1–3]. Carbothermal nitridation eliminates the need for separate synthesis of SiC and subsequent mixing with Si_3N_4.

Because the reaction kinetics of carbothermal Si_3N_4 synthesis are slow, its introduction as a large-scale commercial process has been restricted. Due to the high reaction temperature, a long reaction time makes the carbothermal route energy, and thus, cost intensive. Consequently, a tremendous amount of research has gone into deciphering the reaction mechanism and understanding how the kinetics are affected by both chemistry and various physical parameters [4–10]. If a significant rate enhancement is achieved, carbothermal nitridation will certainly become "the" method for commercial Si_3N_4 production.

1.2. Additives

Licko *et al.* [9] illustrated that SiO_2 reduction is catalyzed by the relatively high concentration of transition metal impurities, such as iron, nickel, and chromium, present in low-grade carbon black. Unfortunately, additions of iron, Fe_2O_3, nickel, and Cr_2O_3, as well as V_2O_5, CaO, MgO, and silicon, have been found to promote both the formation of β-Si_3N_4 and β-SiC [5, 7, 11–13]. Figusch and Licko [7] argue that these impurities form liquid phases that alter the phase equilibria. This in turn changes the thermodynamic activity of the phases and alters the rates of competing reactions. They supported

---

* Author to whom all correspondence should be addressed.

this argument for the case of iron, based on SEM micrographs that showed Fe-rich globules attached to SiC whiskers.

Li *et al.* [14] have demonstrated rate enhancements when rare earth oxides are incorporated into the reactant mixture. They also observed an influence on the α/β ratio and Si_3N_4 particle size. β-Si_3N_4 production was believed to be elevated in cases where a M-Si-O-N (M = rare earth metal) liquid phase formed below the nitridation temperature, which decreased the Gibbs free energy for α to β transformation. In cases where no liquid phase was formed, it was hypothesized that rare earth metal atoms incorporate themselves within the Si-O matrix and catalyze the reduction of SiO_2. Due to the electronegativity difference between Si^{4+} and M^{n+}, the Si-O-M cluster drives electrons to oxygen, which in turn leads to a high potential for M^{n+} to coordinatively bind to a Lewis acid such as CO. They argue that CO can adsorb as CO_3^{2-}, interact with the Si-O-M cluster, and desorb as SiO and CO_2. In support of their theory, rare earth oxide additions caused the IR absorption peak for the Si-O bond to move towards a lower frequency. In other words, the binding constant for Si-O was decreased. They mention the additives must be added to the reactant mixture through a special solgel formulation in order for them to influence the reaction kinetics.

Komeya *et al.* [15] found a number of compounds (rare earth oxides, carbonates, ceramics) to influence the rate of carbothermal AlN synthesis. Calcium fluoride decreased the time to full conversion by 80% and decreased the activation energy from 256 kJ/mol to 187 kJ/mol. Oxides of Cr, Y, Yb and carbonates of Co, Li, Na, and Ni all reduced the time to full conversion from 40–60%. Due to the detection of $CaF_2 \cdot 5Al_2O_3$ and a number of Y-aluminates, along with evidence that their concentration changed with reaction time, these compounds were believed to serve as intermediates, which modify the kinetic mechanism for alumina reduction.

This project expands upon previous work studying the effects of additive on the carbothermal nitridation of SiO_2. We look at the additives used by Koyama *et al.* [15] for A1N reaction enhancement in conjunction with seeding the reaction mixtures with Si_3N_4. Since the nucleation of Si_3N_4 is typically the slow step in the carbothermal synthesis [7], seeding the reagents should increase the rate of reaction. This is an attempt to increase the reaction rate without reducing product quality, as seen in previous studies.

2. Experimental

2.1. Pellet preparation

A homogeneous reactant mixture is produced by milling fine reactant powders for 5 hrs in a Nalgene jar filled halfway with 5-mm hot isostatically pressed (HIPed) silicon nitride media (Azko Nobel). The reactant mixture is composed of carbon, silica, alpha-silicon nitride "seed", wheat starch (Genvis 700, ADM), and corn starch (670, Roquette America, Inc.). The composition is set by the following ratios: mol C/mol SiO_2 = 4 (100% carbon excess), wt. Si_3N_4 "seed"/wt. SiO_2 = 0.1. The weight percentages of wheat and corn starch are 7.5 and 3.1, respectively [16]. The reactant mixture is milled for an additional 3 hours with a 3 wt.% chemical additive (Y_2O_3, Yb_2O_3, La_2O_3, CeO_2, CaF_2, Li_2CO_3, $CoCO_3$, or $NiCO_3$).

To ensure good contacting between the solid and gaseous reactants, the precursor mixture is shaped into cylindrical aggregates so N_2 can flow throughout the sample crucible. To form the reactant pellets, the precursor mixture is first bound together by adding 1 ml of purified, deionized water to every 1.55 g of reactant mixture to activate the starches. The mixture is then thoroughly blended with a mortar and pestle and finally run through an extruder (The Bonnet Co., model M-1), under a pressure of 5.4 Pa (80 psi), into 0.5–1.0 × 10^{-2} m long cylinders with a 0.32 × 10^{-2} m (1/8 in) diameter. Immediately after extrusion, the pellets are dried in an oven for 1 hour at 388 K. Dried pellets are then heated under N_2 at 623–653 K for 3 hours in a tube furnace (Heavy Duty Electric Co., model M3024) to calcine the starch into a high-purity carbonaceous material.

2.2. Reaction apparatus

Synthesis of SiC/Si_3N_4 composite powder is carried out in a custom, high temperature (2573 K capability) Gravitronic VII thermogravimetric analyzer (TGA) (Theta Industries, Inc.) shown in Fig. 1. Samples are held in a high-purity graphite crucible (1.27 × 10^{-2} m (0.5 in) O.D., 2.54 × 10^{-2} m (1.0 in) long) suspended in the

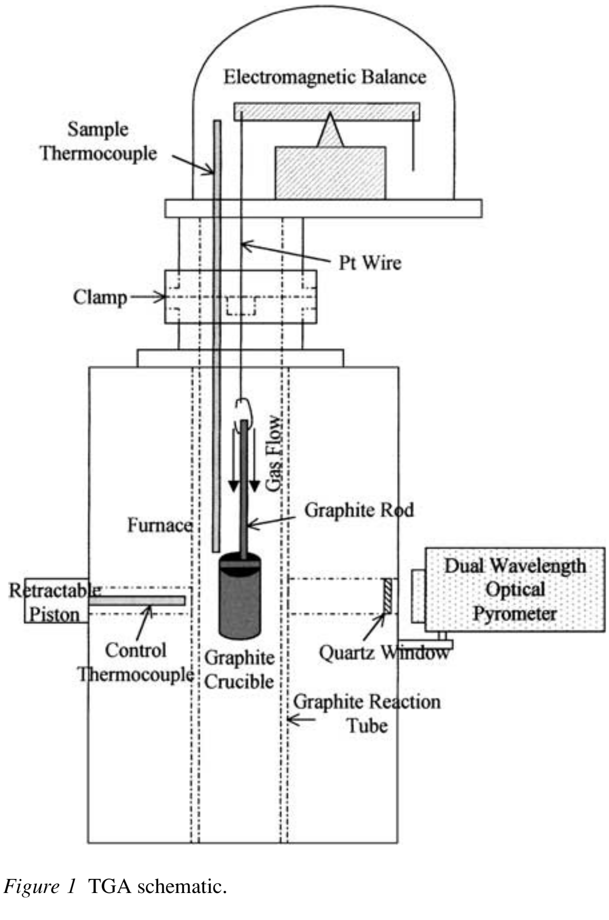

Figure 1 TGA schematic.

center of a vertical graphite tube furnace. The top end of the crucible is open and facing the gas flow that runs down the center of the furnace. Sample weight is monitored with microgram sensitivity via connection to an electromagnetic balance (Cahn Instruments, model D-101). A Eurotherm 2408 temperature controller uses a type S thermocouple or dual wavelength optical pyrometer to maintain the temperature programs. The sample temperature is measured via a second type S thermocouple that hovers over the sample crucible. Samples are heated according to a temperature program set by a software package (Theta Win, version 1.0) interfaced with the instrument. The same software records sample temperature and weight with time. Due to interference caused by removal and reattachment of the sample crucible, the balance is calibrated with a 1 g standard calibration weight (Troemner, Class 1) after approximately every 10 experiments.

2.3. Reaction procedure

The TGA is initially tared with an empty crucible, after which approximately 1.8 g of reactant pellets are loaded into the crucible and the initial sample weight is recorded. Nitrogen is then allowed to run through the furnace at 2.213×10^{-5} m^3/s (1328 cm^3/min). The system is then heated to a desired temperature at a maximum heating rate of 0.5 K/s (30°C/min), where the sample is then either held isothermally for a specified time or run through a nonisothermal temperature program. Once the heating period is finished, the reaction is quenched back to room temperature at a maximum cooling rate of 0.5 K/s (30°C/min). With the gas flow terminated, the final sample weight is recorded. To investigate the effect of each of the selected chemical additives, reaction with each of these materials is carried out at 1748 K for 5 hrs under N_2.

2.4. Post processing

Reacted pellets are gently crushed into a fine powder using a silica mortar and pestle. The powder is then placed into a quartz boat and heated under air in a tube furnace to remove residual free carbon. The sample is heated at 963–1002 K for 3 hrs. Weight measurements are taken before and after carbon burnout using an analytical balance (Mettler, AE160).

2.5. Analytical characterization and data analysis

Carbon and oxygen analyses are carried out using a LECO C200 carbon determinator and LECO TC436DR oxygen determinator, respectively. The LECO data and weight measurements, taken before and after reaction and carbon burnout, are used to calculate a number of quantities to characterize the experiments (weight fractions of reactants and products, yields, selectivity of SiC to Si_3N_4, conversion of SiO_2, and fractional SiO loss). In these calculations, all oxygen present in the precursor and product is assumed to be SiO_2. All carbon in the precursor and burned out product is assumed to be free carbon and SiC, respectively. The SiO_2 and SiC contents in the product could be slightly overestimated due to some oxygen and carbon being present in a Si-O-C phase.

The surface area of product powders is determined by the BET nitrogen adsorption method. Product powder morphology and size are determined by transmission electron microscopy using a JEOL 2010 high-resolution TEM with integrated Oxford Link ISIS energy dispersive x-ray spectroscopy. Particle sizes are determined manually from 20–40 particles on 3–5 TEM images. Energy dispersive x-ray spectroscopy (EDS) is used to assess the composition of particles in the TEM micrographs. The α and β-Si_3N_4 phases are quantified by powder X-ray diffraction (CuKα radiation) using a Scintag PADV powder diffractometer and the method of Gazzara and Messier [17]. Powder X-ray diffraction is also used to verify the presence of SiC.

3. Results and discussion

3.1. Morphology, particle size, and surface area

Eight precursor mixtures, each with a 3 wt.% concentration of a single additive, were reacted at 1748 K for 5 hours, after which the product quality (particle morphology, particle size, surface area, and composition) was examined. Fig. 2 shows product powder TEM micrographs obtained from reactions with each. These photomicrographs suggest that various degrees

TABLE I Product quality as a function of additive

Additive	Wt.% Si_3N_4	$\alpha/(\alpha+\beta)$ %	Wt.% SiC	Wt.% O	Wt.% C	Particle size α-Si_3N_4 (μm)/ β-SiC (μm)	Surface area (m^2/g)
none	94.0	>95	1.9	1.8	0.5	0.6-0.3/NA	11.9
CeO_2	84.6	>95	3.3	5.7	0.9	0.5-0.3/<0.080	8.3
La_2O_3	90.0	>95	4.9	2.4	1.3	0.6-0.3/<0.080	5.7
Yb_2O_3	92.5	86.4	3.2	2.0	0.8	0.6-0.3/<0.100	5.2
Y_2O_3	91.4	85.6	4.4	2.0	1.2	0.6-0.1/<0.050	8.9
CaF_2	82.0	87.8	12.4	2.6	3.2	0.6-0.2 /<0.050	8.1
$CoCO_3$	22.1	>95	69.7	3.8	18.2	0.4-0.1/<0.100	3.6
Li_2CO_3	92.5	>95	3.2	2.0	0.8	0.6-0.3/<0.080	8.5
$NiCO_3$	31.5	73.2	63.1	2.5	16.5	0.5-0.1/<0.100	12.6

Reaction conditions: temp = 1475°C; time = 5 hrs.; atmosphere = N_2. Precursor composition: $C/SiO_2 = 4$ (molar ratio); $Si_3N_4/SiO_2 = 0.1$ (weight ratio); 3 wt.% additive.

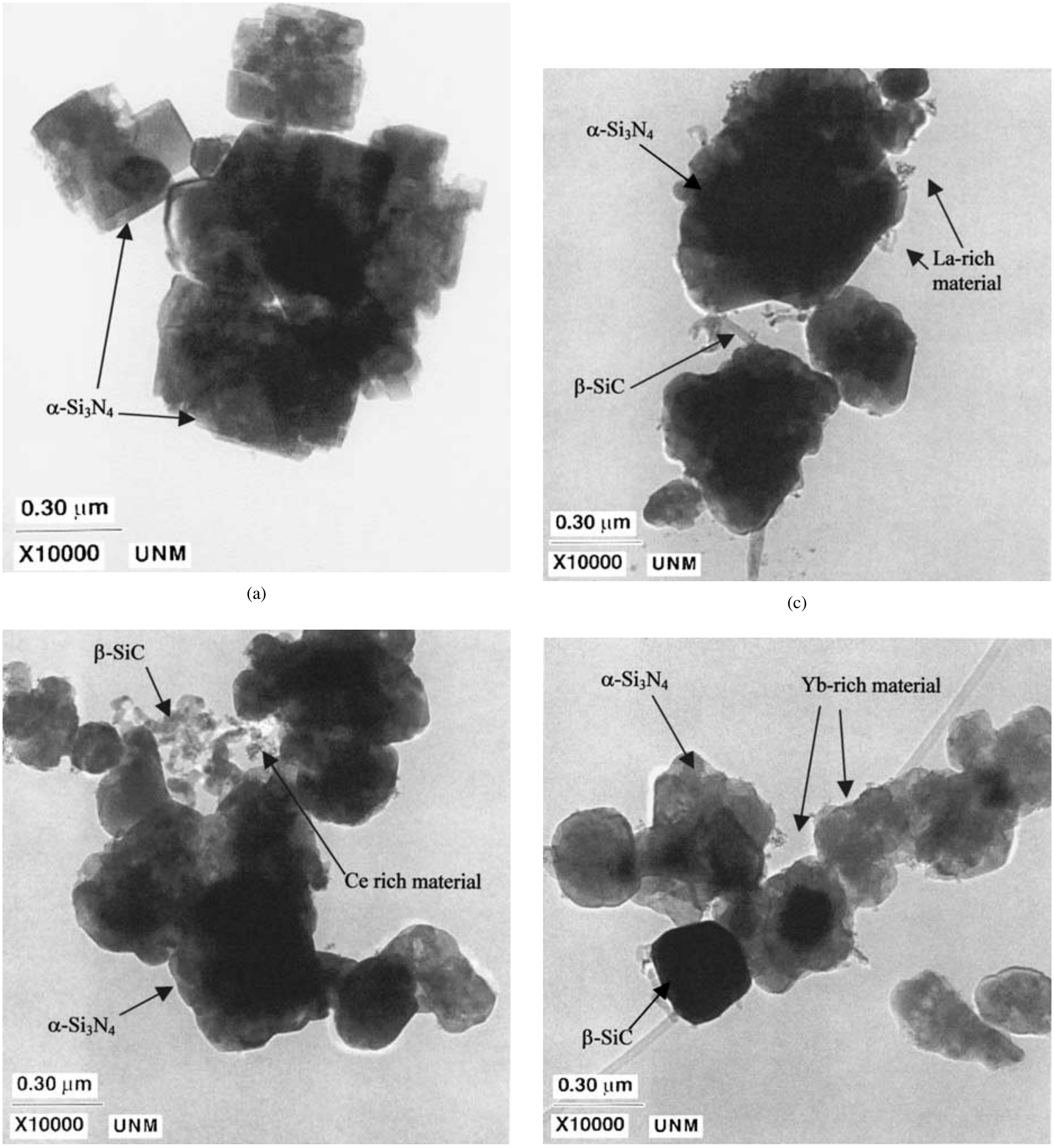

Figure 2 TEM micrographs of product powders obtained under various additives. Reactions conditions: 1748 K; 5 hours. Precursor composition: $C/SiO_2 = 4$ (molar ratio); $Si_3N_4/SiO_2 = 0.1$ (weight ratio); 3 wt.% addition of (a) no additive, (b) CeO_2, (c) La_2O_3, (d) Yb_2O_3, (e) Y_2O_3, (f) CaF_2, (g) $CoCO_3$, (h) Li_2CO_3, (i) $NiCO_3$ *(Continued)*.

of sintering take place under all of the additives except Li_2CO_3. The product obtained under Li_2CO_3 is similar to that produced in the absence of additive in that highly faceted α-Si_3N_4 crystals were formed. The aggregated morphology associated with the rest of the additives indicates the presence of a liquid phase during product formation. This is surely the case for yttria and calcium fluoride since these materials are commonly used as sintering aids for Si_3N_4 ceramics. For nickel and cobalt carbonate, liquid phase formation is further supported by evidence of a thin coating of a secondary material around various particles. This coating could very well have resulted from liquid solidification. The EDS spectra for the $CoCO_3$ sample (Fig. 3) showed significant levels of Co. Iron is known to form a liquid phase during carbothermal nitridation of silica. Given their placement in the periodic table, it is reasonable to assume that cobalt and nickel share similar affinities to form low-melting eutectic phases with other species present in the reactant mixture.

Additives generally led to a decrease in surface area relative to that achieved without additive (Table I). La_2O_3, Yb_2O_3, and $CoCO_3$ led to reductions in surface area of 50 to 60%. This is undesirable with respect to the formation of mechanical components. Low surface area materials do not densify well and thus lead to

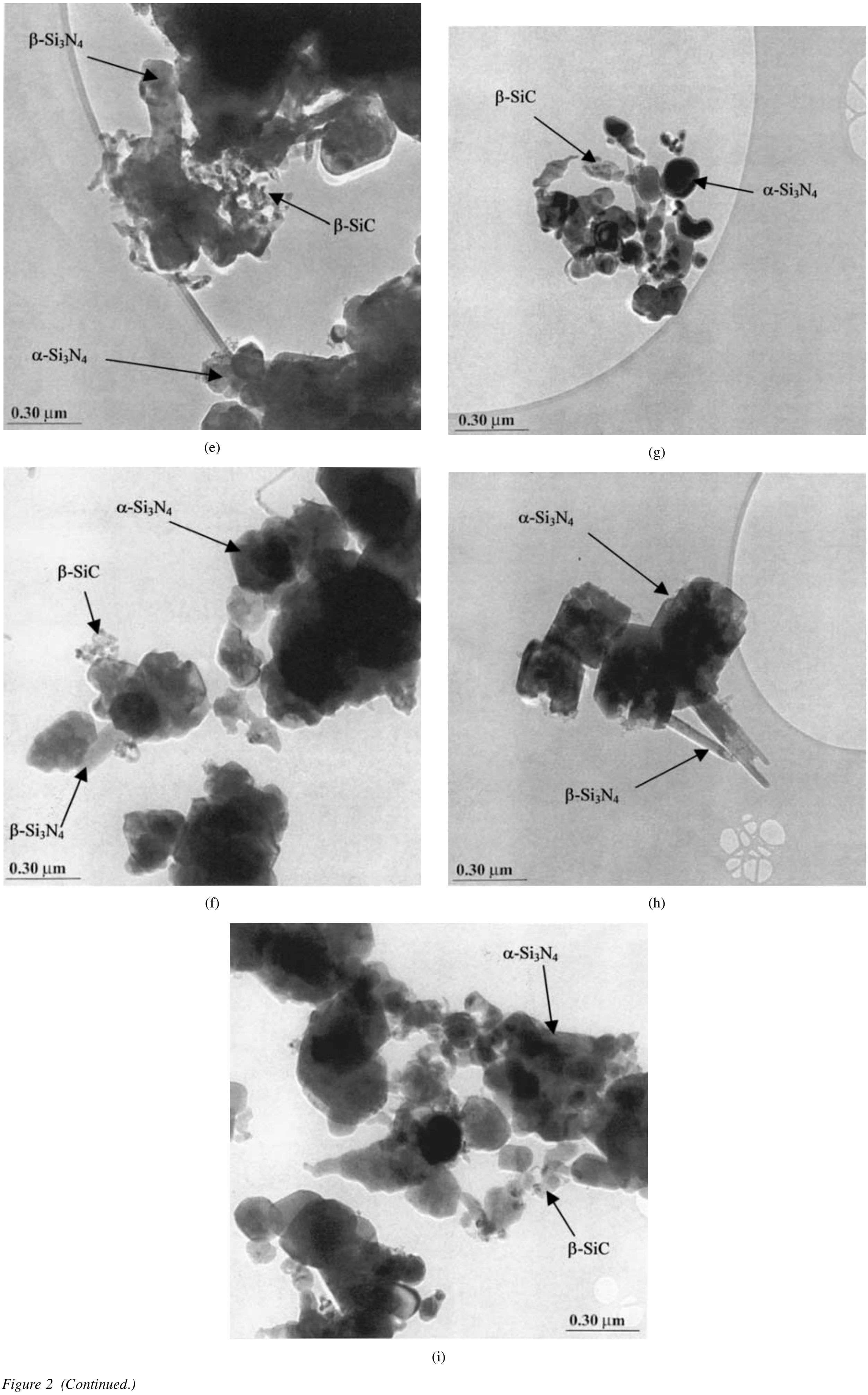

(e) (g)

(f) (h)

(i)

Figure 2 (Continued.)

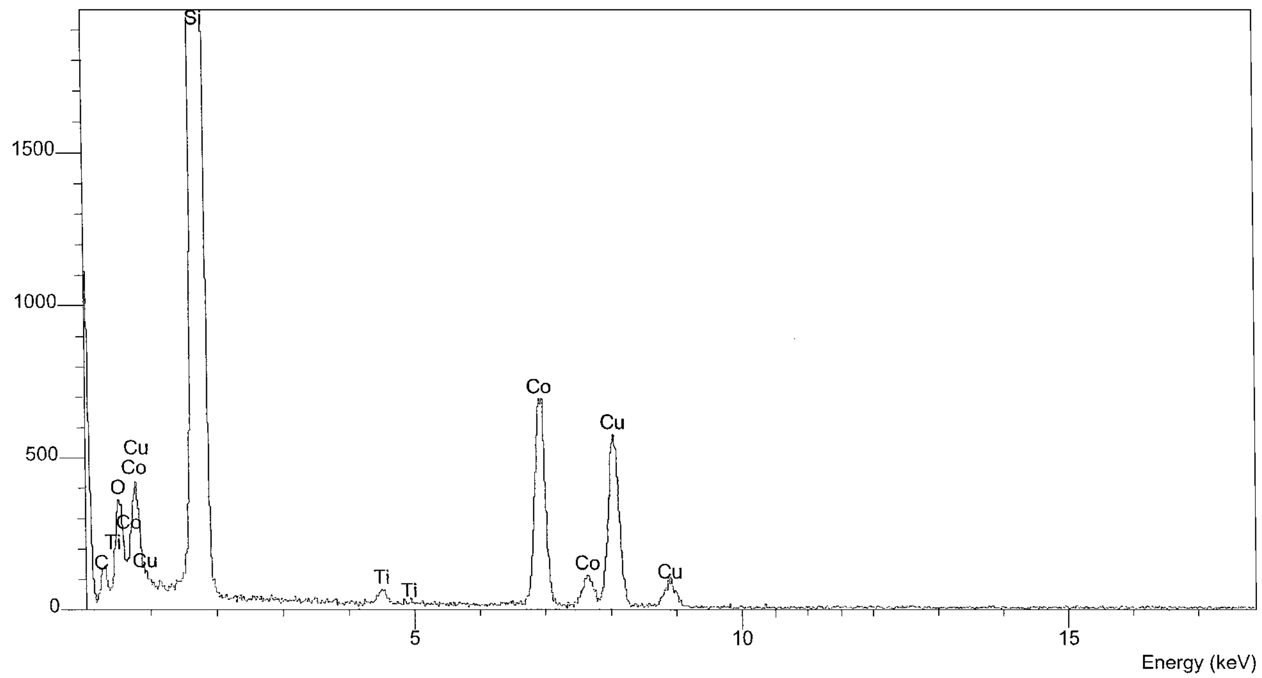

Figure 3 EDS spectrum for sample with $CoCO_3$ promoter. This shows significant levels of Co in the sample. The copper peaks are from the copper grid upon which the samples were placed for imaging and analysis. The titanium peaks are from the chamber in which the analysis was performed.

inferior mechanical properties. Given that the particle sizes did not vary greatly with additives (Table I), the decrease in surface area could be partially attributed to a lower degree of surface irregularity caused by liquid formation or a partial sintering of the product. Although $NiCO_3$ gave an agglomerated product, its surface area was a bit greater than that obtained without additive. This stems from an extremely high content of nanophase SiC (Table I). $CoCO_3$ led to an equally high nanophase SiC content, however, the surface area was only 3.6 m^2/g. The particles produced with $CoCO_3$ must have little surface irregularity. A high degree of liquid formation could have been responsible for this effect.

Aside from the cobalt and nickel carbonate experiments; there was little variance in α-Si_3N_4 particle size among the samples with and without additive. All of the precursor mixtures contained α-Si_3N_4 seed, hence particle size was not dependent on nuclei formation, and was only a function of the fraction of silicon atoms that went towards α-Si_3N_4 growth. Runs that produced similar α-Si_3N_4 contents therefore shared the same range in α-Si_3N_4 particle size (Table I). For samples with a significant β-Si_3N_4 and/or β-SiC content, the range in α-Si_3N_4 particle size was reduced. In these cases, a smaller fraction of silicon atoms went towards α formation, thus α crystallite growth was abated. This effect is prevalent in the case of cobalt and nickel carbonate due to the high β-SiC contents produced. All SiC detected by TEM was on the nanometer scale. Due to the small size of this material and a limited number of micrographs, differences in SiC particle size could not be assessed.

Most of the samples contained a minute quantity of fine fluff around the Si_3N_4 and SiC product. This material was examined by EDS and determined to contain silicon, oxygen, and carbon. This type of Si-O-C phase was also observed by Weimer *et al.* [10], and is believed to be an intermediate phase to α-Si_3N_4. The near absence of this phase in the CaF_2, $CoCO_3$, and $NiCO_3$ runs explains the reduced α-Si_3N_4 content associated with these additives. For the cases of CeO_2, La_2O_3, and Yb_2O_3, EDS showed the fluff to be rich in the rare earth oxide (Fig. 4). For the carbothermal nitridation of Al_2O_3, Komeya *et al.* [15] observed yttrium aluminates when Y_2O_3 was added to the reaction mixture. The addition of this material led to a rate enhancement, and it was reasoned the aluminates had a catalytic effect on the formation of AlN. The rare earth—rich fluff found in this study could be made up of rare earth silicates that offer the same benefit.

3.2. Product distribution

Table I shows that additives generally resulted in a subtle increase in oxygen content. Since the reaction rate was significantly enhanced by all of the additives, it is unlikely this elevation in oxygen is due to unreacted silica. Given the reducing nature of metallic elements, the metals associated with the additives are sure to have caused retainment of oxygen in the sample. Due to the abnormally high oxygen content associated with CeO_2, cerium must have an advanced effect on the retainment of oxygen.

An increase in SiC was also observed with the addition of additive. Lithium carbonate and the rare earth oxides provided a slight enhancement in this quantity, which is desirable with respect to nanophase SiC/Si_3N_4 composites. A percentage of SiC greater than 10 wt.% substantially inhibits sinterability when densifying

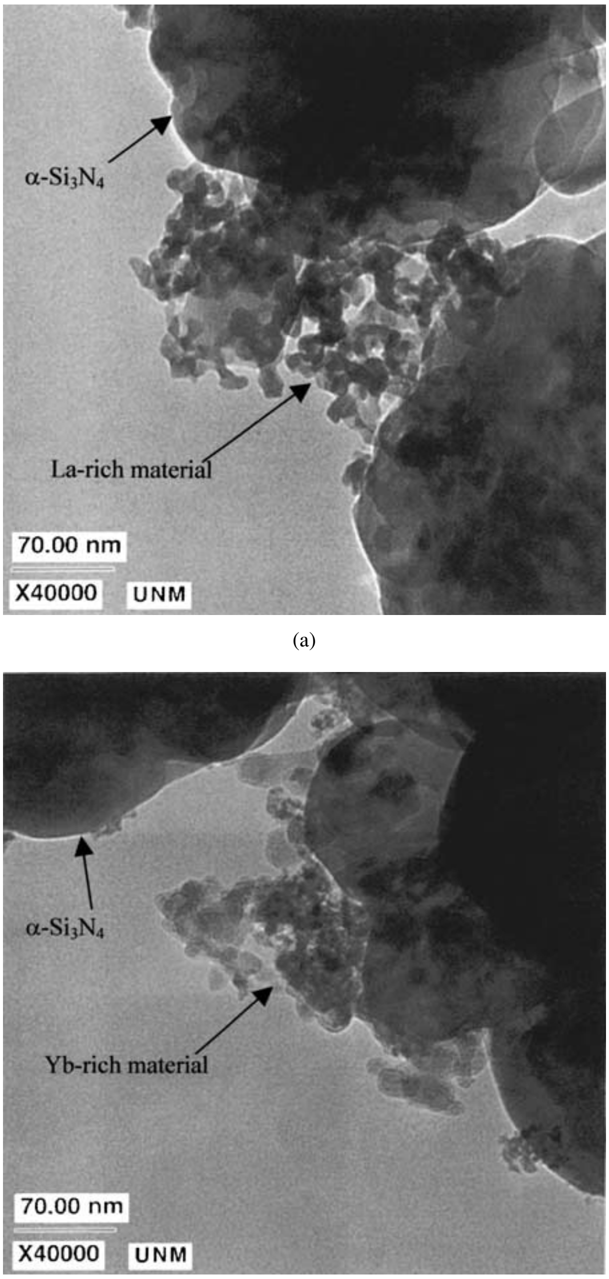

(a)

(b)

Figure 4 TEM micrographs of rare earth-rich Si-O-C phases observed in product powder. Reaction conditions: 1475°C; 5 hours. Precursor mixture: $C/SiO_2 = 4$ (molar ratio); $Si_3N_4/SiO_2 = 0.1$ (weight ratio); 3 wt.% a) La_2O_3, b) Yb_2O_3.

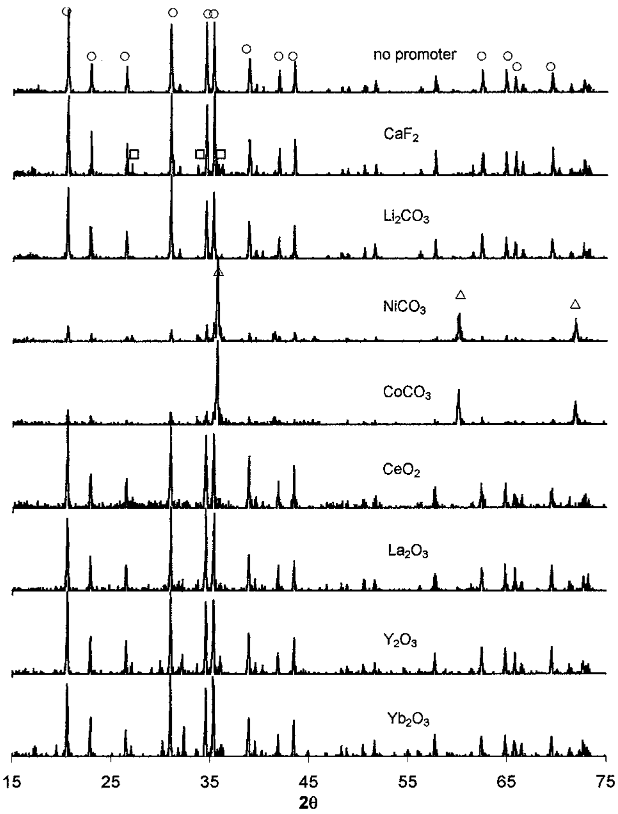

Figure 5 Powder x-ray diffraction data for products obtained under various additives. Reaction conditions: 1475°C; 5 hours; N_2 atmosphere. Precursor composition: $C/SiO_2 = 4$ (molar ratio); $Si_3N_4/SiO_2 = 0.1$ (weight ratio); 3 wt.% additive (given as title is above charts). Key: α-Si_3N_4—circles; β-Si_3N_4—squares; β-SiC—triangles. The peaks are identified on the uppermost diffraction pattern on which they appear.

components. The addition of CaF_2 caused a more significant increase. This is in agreement with Peck *et al.* [11], in that calcium compounds tend to appreciably promote β-SiC formation. Although there were no resolved β-SiC peaks in the x-ray diffraction pattern, β-SiC was detected by TEM. It is possible that either the size and/or quantity of SiC made x-ray detection difficult. Since CaF_2 is a common sintering aid, it is highly probable that SiC formation was promoted through a liquid phase contrived by the additive. Cobalt and nickel carbonates both imposed a tremendous SiC favorability over Si_3N_4, in that both additives led to a SiC content over 60 wt.%. X-ray diffraction validated the predominance of β-SiC. Although nothing has been reported regarding cobalt compounds, nickel has demonstrated an enhancement to both β-SiC and β-Si_3N_4 formation [11]. The liquids that form from these compounds may alter silica reduction in such a way as to inhibit the production of Si_3N_4-forming intermediates. Iron has been shown to promote the SiC content through formation of a low-melting eutectic phase [12]. Once again, the similarity among iron, cobalt, and nickel likely originates from the common chemistry shared by these transition metals. When comparing carbonates, Li_2CO_3 had quite a different effect on the system. This is sure to stem from differences in chemistry between transition metal and alkaline earth species.

Fig. 5 displays the powder x-ray diffraction patterns related to the samples in Table I. Silicon nitride was obviously the dominant phase for all of the samples excluding those with $CoCO_3$ and $NiCO_3$. Yb_2O_3, Y_2O_3, CaF_2, and $NiCO_3$ addition resulted in product powder with measurable β-Si_3N_4 peaks. The presence of β-Si_3N_4 in Y_2O_3 and CaF_2 samples makes sense from the standpoint that these compounds are frequently used to sinter Si_3N_4 and promote α to β-phase transformation. Whether the formation of β-Si_3N_4 is solely due to sintering of the α product or, in part, the result of a change in reaction chemistry, has yet to be determined. Although Li *et al.* [14] observed greater β contents for 0.5 wt.% CeO_2, La_2O_3 and Y_2O_3 additions; their reaction system did not contain α-Si_3N_4 seed. The results of this study suggest that seeding has a counteractive effect on β-phase formation. Additives that promote undesirable β-Si_3N_4 formation are, therefore, not necessarily a poor choice. Akin to iron compounds, $NiCO_3$ encouraged β-Si_3N_4 development. Cobalt carbonate would be expected to follow suit. However, there were no β-Si_3N_4 peaks present in the x-ray pattern for the $CoCO_3$ containing reacted sample. This is perhaps due to the low Si_3N_4 content.

3.3. Mechanism

The rare earth oxides shared similar effects on both product quality and reaction rate. It is therefore plausible to believe these compounds alter Si_3N_4 synthesis by a common mechanism. These additives may enhance the rate of Si_3N_4 production by forming a chemical bridge between carbon and silica. Carbon would have a tendency to reduce the rare earth oxide while the rare earth element itself would have a tendency to reduce silica. The result of such a mechanism would lead to a rare earth-rich Si-O-C phase, which could go on to interact with N_2 and form Si_3N_4. The cycle would regenerate itself in that silicon, carbon, and oxygen would be fed to the intermediate phase, as these elements are lost as Si_3N_4(s) and CO (g). Energy dispersive x-ray spectroscopy analysis did detect an intermediate rare earth – rich Si-O-C phase for the CeO_2, La_2O_3, and Yb_2O_3 runs. This agrees with Komeya *et al.* [15], who found the addition of Y_2O_3 to the reactant mixture for carbothermal AlN synthesis led to several Y-aluminates. It is possible that the extraneous peaks associated with the Yb_2O_3 and Y_2O_3 runs of the study represent Yb and Y-silicates, respectively.

The agglomerated particles that were produced with the rare earth oxides are indicative of a liquid phase present during synthesis. Melting of the M-Si-O-C (M = rare earth metal) phase would enhance silicon, oxygen, and carbon transport and, thus, lead to an enhanced reaction rate and agglomerated product particles. The difference in β-Si_3N_4 content among the rare earth oxides is possibly due to various degrees of eutectic formation.

Calcium fluoride promotes a radical increase in the rate of conversion of silica to silicon nitride. This may stem from the high reduction potential of calcium. In light of the fact that this additive is a common sintering aid, liquid formation is sure to have occurred. The heightened β-Si_3N_4 content associated with CaF_2 may be due to heightened eutectic formation.

Lithium has a large reduction potential similar to calcium, hence the rate of silica conversion with these two additives is equal during the first 30 minutes of reaction at 1748 K. The rate of Si_3N_4 synthesis under Li_2CO_3 is a bit peculiar, however, in that the rate drops dramatically after this initial period. It is possible that silica is rapidly reduced by lithium into an intermediate, whose conversion to Si_3N_4 is sluggish.

Cobalt and nickel carbonates intensified silica reduction as well as β-SiC formation. The behavior of cobalt and nickel is analogous to iron. The chemistry of these transition metal atoms has a definite effect on the interaction of N_2 with the intermediates that are formed from these metals. How this occurs is something that needs further investigation. All of these transition metals from liquid intermediates, and it is possible that the flux of N_2 into these intermediates is inhibited by physical and/or chemical properties associated with the liquid. This could therefore lead to a decrease in Si_3N_4 formation.

4. Conclusions

The rate of carbothermal nitridation of silica can be promoted by adding compounds commonly used as sintering aids. All of the additives tried in this study decreased the time to complete reaction. All of these additives affect the product quality in different ways. However, lithium carbonate appeared to produce the product with the best quality, high α/β ratio, high surface area, good SiC content, and low residual oxygen. The promoters appear to work based on forming liquid eutectic phases, which provide a lower energy path for the reduction, however more work is needed to identify the mechanism for reaction promotion.

Acknowledgement

The authors are grateful for financial support provided through NSF Grant CTS-9803539. The TEM/EDS work was conducted at the Transmission Electron Microscopy Laboratory in the Department of Earth and Planetary Sciences of the University of New Mexico.

References

1. M. HERRMANN and C. SCHUBER, *J. Am. Ceram. Soc.* **81** (1998) 1095.
2. M. HERRMANN and C. SCHUBERT, *ibid.* **81** (1998) 1109.
3. K. NIIHARA, US Patent No. 5,134,097, (1992).
4. S. BANDYOPADHYAY and J. MUKERJI, *Ceramics International* **17** (1991) 171.
5. Y. W. CHO and J. A. CHARLES, *Mater. Sci. Technol.* **7** (1991) 289.
6. M. EKELUND, *Chemical Communications Stockholm University* **4** (1991) 1.
7. V. FIGUSCH and T. LICKO, In "High Tech Ceramics," edited by P. Vincenzzini (Elsevier Science Publishers B. V. Amsterdam, 1987).
8. T. LIOU and F. CHANG, *Ind. Eng. Chem. Res.* **34** (1995) 118.
9. T. LICKO, V. FIGUSCH and J. PUCHYOVA, *J. Eur. Ceram. Soc.* **9** (1992) 219.
10. A. W. WEIMER, G. A. EISMAN, D. W. SUSNITZKY, D. R. BEAMAN and J. W. McCOY, *J. Am. Ceram. Soc.* **80** (1997) 2853.
11. D. H. PECK, J. Y. KIM and S. W. CHOI, *Key Engineering Materials* **89–91** (1994) 15.
12. S. A. SIDDIQI and A. HENDRY, *J. Mater. Sci.* **20** (1985) 3230.
13. A. W. WEIMER, *J Mater. Sci. Lett.* **17** (1998) 123.
14. W. LI, Y. ZHUANG and G. SUN, *J. Rare Earths* **14** (1996) 128.
15. K. KOMEYA, E. MITSUHASHI and T. MEGURO, *J. the Ceram. Soc. Jpn* **101** (1993) 377.
16. A. W. WEIMER and K. J. NILSEN, US Patent No. 5,384,291, (1995).
17. C. P. GAZZARA and D. R. MESSIER, *Ceramics Bulletin* **56** (1977) 777.

Received 30 June
and accepted 26 December 2000